

Effects of the spray angle on splat morphology during thermal spraying

G. Montavon ^{a,*}, S. Sampath ^b, C.C. Berndt ^b, H. Herman ^b, C. Coddet ^a

^a *Laboratoire d'Etudes et de Recherches sur les Matériaux et les Propriétés de Surface, Institut Polytechnique de Sévenans, BP 449, 90 010 Belfort, Cedex, France*

^b *The Thermal Spray Laboratory, Department of Materials Science and Engineering, State University of New York at Stony Brook, Stony Brook, NY 11794-2275, USA*

Received 1 July 1996; accepted 30 September 1996

Abstract

The effects of spray angle on the morphology of thermally sprayed particles impinging on polished substrates have been studied by implementing several statistical tools (i.e., Gaussian analysis, Weibull distribution and the t-test). Nickel-based alloy (Astroloy) particles were vacuum plasma-sprayed onto copper plates at normal (i.e., 90°) and several off-normal spray angles (i.e., 75, 60, 45 and 30°). Different geometric shape factors (i.e., referring to an equivalent diameter, elongation factor and degree of splashing) were determined using image analysis. The spray angle had a strong effect on these geometric properties, in particular on the elongation factor of the shapes.

Keywords: Vacuum plasma spraying; Spray angle; Droplet; Statistical analysis; Image analysis; Deposition efficiency

1. Introduction

Mechanical, thermo-physical, and other properties of thermally sprayed coatings are controlled by the impingement, spreading and solidification of discrete molten or semi-molten particles on a substrate or previously deposited layers [1]. However, the relationships between the parameters (i.e., impact velocity of the droplets, temperature and viscosity of the molten particle, substrate temperature, etc.) and the morphology of splats are not well known. Difficulties in experimentally measuring or numerically modeling these factors have impeded the understanding of the impact mechanisms until recently where researchers have started to measure [2–4], or model [5–7], these phenomena. Among influential parameters, the spray angle has received only little attention. Recent papers [8,9] have emphasized the significant effects of an off-normal spray angle on characteristics of HVOF (high velocity oxygen-fuel) and VPS (vacuum plasma spraying) sprayed deposits; in particular the drastic decrease of deposition efficiency and the increase of the porosity, below a certain spray angle.

The aim of this work was to analyze the effects of the spray angle on the geometric characteristics of Astroloy

particles after their impingement on a smooth substrate by implementing several statistical tools, such as Gaussian analysis, Weibull distribution analysis and the t-test. This study complements another paper [10] dealing with the effects of processing parameters, such as arc intensity, and plasma gas mass flow rates, on the splat morphology.

2. Experiments

2.1. Material characterization

The feedstock material used to perform this study was a nickel-based alloy, named Astroloy. The composition of this material is listed in Table 1 and the particle size distribution is shown in Fig. 1. The powder is characterized by near-perfect spherical particles, as illustrated in Fig. 2; such a typical shape being obtained from the gas atomization process. In the following description, the spray angle is defined as the angle between the axis of the plasma gun and the surface of the substrate, in the plane orthogonal to the gun displacement (Fig. 3). Five different spray angles were tested: 90, 75, 60, 45 and 30°.

* Corresponding author. Tel.: +33 84 583051; fax: +33 84 583030.

Table 1
Chemical composition of Astroloy^a

Element	Weight (%)	Element	Ppm
Ni	Balance	B	2000
Co	18.80	C	2000
Cr	14.90	Si	2000
Mo	4.99	O	85
Al	3.99	N	29
Ti	3.55	S	5
Fe	0.11		
Zr	0.04		

^aManufacturer's specifications (Tecphy, France): powder referenced PY158 (Astroloy for thermal spraying) produced by gas atomization.

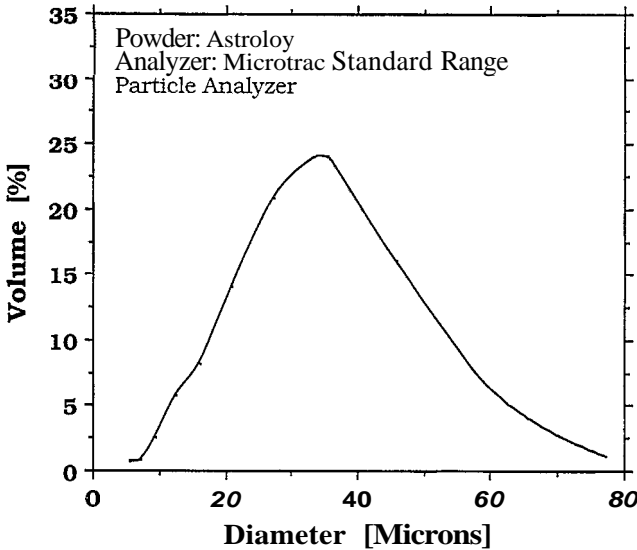


Fig. 1. Grain size distribution of Astroloy.

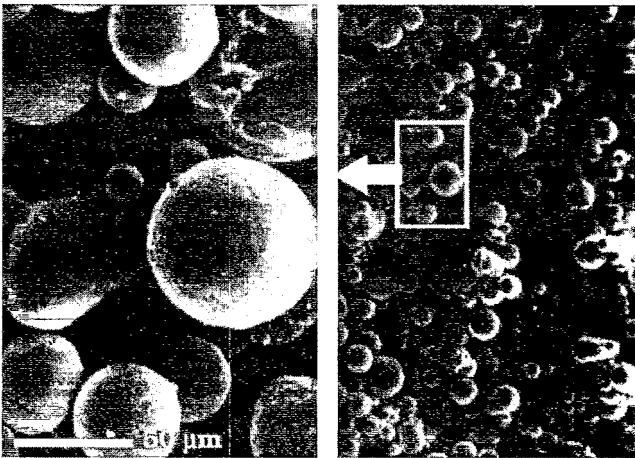


Fig. 2. SEM view of the Astroloy powder particles

2.2. Spray conditions

The particles were sprayed on polished copper substrates, prepared by grinding with 600 grit SiC paper

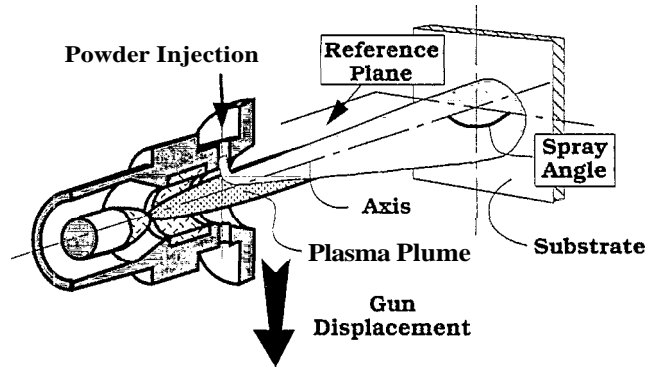


Fig. 3. Experimental set-up to perform the tests,

and followed by 5, 1 and 0.1 μm diamond slurry polishing. After polishing, the substrates exhibited surface roughnesses (e.g., rms) ranging from 0.1 to 0.3 μm .

The powder was vacuum plasma spray (VPS) processed, at a chamber pressure of 60 mbar, in an inert residual atmosphere of argon, using a PT-VPS A-2000 system with an F4-VB torch. The main spray parameters are listed in Table 2. The plasma gun moved at a velocity of 1 m min^{-1} for one pass accomplished in front of each substrate. The gun displacement was normal to the reference plane. In such a way, possible distortions of splats induced by the gun displacement do not interfere with those induced by the spray angle. Moreover, due to the relatively short interaction time between the substrate and the heated gases (i.e., approximately 3 s), it is considered that the substrate temperature is not modified, and is kept constant and equal to the room temperature (e.g., 293 K).

At low pressure and when the atomic/molecular mean free path over the particle diameter ratio becomes higher than 0.01, it is known that the Knudsen effect, or "rarefaction" effect, may significantly reduce the heat flux from the plasma plume to small particles and the drag coefficient [11]. Hence, the Knudsen effect increases: (i) when decreasing the particle size [12]; and (ii) when increasing the surface temperature of the particles [13]. Considering thermal plasmas, this effect is emphasized for small diameter particles: lower than 10 μm [11–14]. In the following comments, this phenomenon will not be taken into account, due to the particle size distribution of the Astroloy powder: less than 2.5%

Table 2
Spray parameters

Plasma gun	PT F4
Argon mass flow rate	50 l min^{-1}
Hydrogen mass flow rate	8 l min^{-1}
Current intensity	700 A
Chamber pressure	60 mbar
Powder carrier gas mass flow rate	3.4 l min^{-1}
Powder feed rate	3 g min^{-1}

(by volume) of the particles exhibit diameters smaller than 10 μm .

2.3. Image analysis

The splat characteristics were measured using optical microscopy coupled with image analysis [9, 10]. Different shape factors were used in order to quantify the phenomena; in particular the equivalent diameter, E.D., defined as the diameter of a circle with the same area as the selected feature; the elongation factor, E.F., defining the non-circular nature of a selected feature, unity being a perfect circle; and the degree of splashing, D.S., characterizing the importance of the splashing phenomenon (i.e., peripheral projection of material at the impact); unity resulting from an absence of such projections. Eqs. (1)–(3) present the mathematical definitions of these shape factors [10], schematically illustrated in Fig. 4.

$$\text{equivalent diameter, E.D.} = \left(\frac{4 \cdot A}{\pi} \right)^{1/2} \quad (1)$$

$$\text{elongation factor, E.F.} = \frac{n}{4} \cdot \frac{L^2}{A} \quad (2)$$

$$\text{degree of splashing, D.S.} = \frac{1}{4\pi} \cdot \frac{P^2}{A} \quad (3)$$

where A is the area of the selected feature, L is the longest dimension and P is the perimeter.

Due to its mathematical definition, the degree of splashing, D.S., is correlated to the elongation factor,

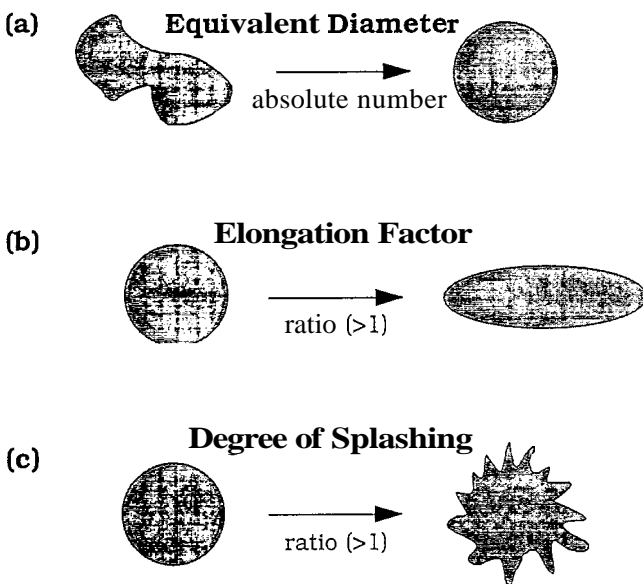


Fig. 4. Equivalent diameter, elongation factor and degree of splashing of a selected feature.

E.F. Hence, highly elongated splats will be characterized by artificially high degrees of splashing. The corresponding data have to be corrected, as illustrated in Fig. 5.

Each measurement series of 50 readings were randomly located. The resulting data were adjusted by subtracting the two largest and the two smallest data points to discriminate against atypical values. The presented results refer to the adjusted data.

3. Statistical analysis

Several statistical analyses were performed on the collected data. The following outline provides basic information about these statistical treatments [10].

- (1) The estimation of the data scatter was determined using the mean value, μ , and the standard deviation, σ , of the Gaussian distribution.
- (2) The estimation of the variability within the distributions was made by calculating the Weibull parameters (i.e., Weibull modulus, m , and characteristic value, x), which respectively reflects the data scatter within the Weibull distribution and gives the 63.2% percentile of the cumulative density. Determination of these parameters was accomplished by a curve-fitting method.
- (3) The data were discriminated using the t-test. This statistical procedure compares the hypothesis that the means of data sets are, or are not, identical; assuming that the sample populations of the data sets belong to a Gaussian distribution.

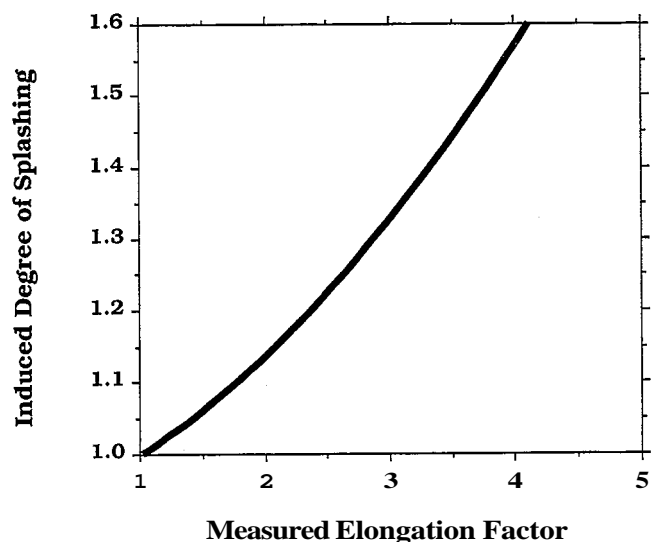


Fig. 5. Correction factor applied to the degree of splashing, as a function of the elongation factor.

4. Results and discussion

4.1. Optical observation

Fig. 6 illustrates the evolution of the morphology of splats when the spray angle changes from 90 to 30°. The "pancake shape" indicates, in both cases, a relatively homogeneous molten state of the impinging particles before the impact [15]. A clear elongation of the splat appears when the spray angle decreases. The peripheral projection of material (i.e., splashing) is randomly distributed with a 90° spray angle and becomes oriented following the impact direction with an off-normal spray angle.

4.2. Gaussian analysis

The results of the Gaussian analysis are listed in Table 3. Fig. 7 shows the Gaussian statistics (arithmetic average and standard deviation represented by an error bar) relative to the data collected according to the

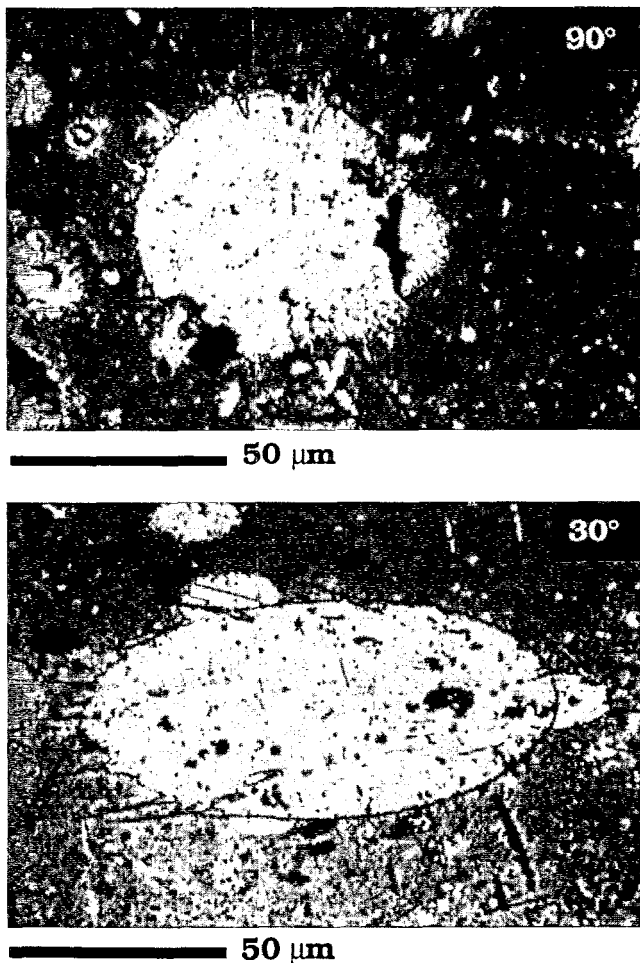


Fig. 6. Morphologies of individual splats for 90 and 30° spray angles.

experimental conditions described earlier. The examination of these results indicates the following:

- (1) The spray angle (Fig. 7(a)) does not significantly influence the arithmetic average of the equivalent diameter. Typically, the arithmetic average of the equivalent diameter fluctuates from 77 to 99 μm .
- (2) The elongation factor of the splats (Fig. 7(b)) is the most affected shape factor, increasing approximately from 1.3 to 2.1 when the spray angle changes from 90 to 30°, indicating a distortion of the shape following the impact direction. Moreover, the standard deviation decreases with a decrease of the spray angle.
- (3) There is no clear trend of the degree of splashing with respect to the spray angle (Fig. 7(c)), except a significantly greater data scatter at spray angles less than 45°. The variance changes from about 19 to 35%.

Correlations between the different shape factors can be also considered. Fig. 8 shows the evolution of the degree of splashing as a function of the equivalent diameter of splats for two spray angles (i.e., 90 and 30°). The smaller the equivalent diameter of the splat, then the lower is the associated splashing phenomenon. This behavior is not influenced by the spray angle, the tendency being practically identical in both cases, although greater in the case of off-normal spray angles.

On the other hand, an increase of the elongation factor corresponds to a significant increase of the splashing phenomenon. This phenomenon is particularly pronounced in the case of the normal spray angle (Fig. 9). Two major reasons may lead to such a behavior. On the one hand, it may be induced by a different spreading process of the particle; i.e., substitution of a radial and equally distributed flow with a normal spray angle to an oriented flow with an off-normal spray angle. On the other hand, a more narrow-sized particle size distribution forms the splats of smaller diameters obtained with an off-normal spray angle, compared to the normal one (Section 4.5). In that case, the previously described influence of the equivalent diameter on the degree of splashing may play its full role.

4.3. Weibull analysis

Weibull moduli, m , and characteristic values, x_0 , relative to the distributions of the data sets were determined (Table 4).

Considering the equivalent diameter, the calculated Weibull moduli can be classified as low (between 2.1 and 3.5) for the distributions, indicating a large variability in the data equivalent to those measured earlier [10] with different processing parameter sets. It can be considered that this shape factor is insensitive to the spray

Table 3
Flattened particle characteristics

Test	E.D. (mm)			E.F.			D.S.		
	μ	σ	σ/μ	μ	σ	σ/μ	μ	G	σ/μ
90°	0.090	0.033	0.366	1.37	0.12	0.08	2.00	0.39	0.19
75°	0.080	0.043	0.537	1.40	0.13	0.09	1.89	0.40	0.21
60°	0.090	0.033	0.366	1.62	0.26	0.16	1.83	0.38	0.21
45°	0.077	0.024	0.311	1.74	0.23	0.13	1.93	0.42	0.22
30°	0.099	0.041	0.414	2.10	0.29	0.14	1.99	0.71	0.35

E.D., equivalent diameter; E.F., elongation factor; D.S., degree of splashing.

angle and essentially depends on the particle size distribution of the powder.

For the elongation factor, the Weibull moduli relative to the distributions can be classified as relatively high (between 7.8 and 12.4), indicating a small variability of the data. However, a general trend indicates that the lower the spray angle, the lower the Weibull modulus and the higher the variability of the corresponding data.

Considering the degree of splashing, the calculated Weibull moduli can be classified as low (between 3.3 and 5.8) for the distributions, indicating significant variability in the data. The relatively low value in the case of the 30° spray angle (i.e., $m=3.3$) relates to a high variability of the corresponding data and may indicate a change in the spreading process at low spray angles.

4.4. *t*-test analysis

The *t*-test protocol was also used to discriminate the data but little new information appeared from this procedure (Table 5).

For the equivalent diameter, the data sets exhibit similarities among themselves, corresponding to a relative insensitivity of the splat equivalent diameters to an evolution of the spray angle.

For the elongation factor, significant variations characterize the data sets, confirming sensitivity of the elongation factor of the flattened particles to any variation of the spray angle.

The data relative to the degree of splashing of splats sprayed with an off-normal angle are similar among themselves and different from the normal angle data, since the splashing changes from a random distribution (normal spray angle) to an oriented distribution (off-normal spray angle).

4.5. Geometric relationships

Geometric relationships between the initial diameter of an impinging particle and the diameter and the thickness of the resulting splat can be heuristically defined following two separated approaches. The first

model is based on Madejski's relationships and assumes a constant degree of splashing of particles (i.e., discrete model). The second model is based on relationships between the initial particle size distribution and the splat equivalent diameter distribution (i.e., probabilistic model). Any specific value of the degree of splashing of particles is postulated in this second case. In both models, it is assumed that: (i) there is no partial vaporization of the particles during their flight in the plasma plume (mass conservation between an initial particle and the resulting splat); (ii) a complete vaporization of particles can occur, inducing their disappearance; and (iii) the splat thickness exhibits a near-constant value along a random cross-section. In the following, the models are successively presented and the results are discussed.

4.5.1. Discrete model

Madejski's relationships [16], among others [3,17], define geometric links between the diameter of an impinging particle and the diameter and the thickness of the resulting splats as follows:

$$D = 1.29 \cdot d \cdot \text{Re}^{0.2} \quad (4)$$

$$H = \frac{2}{3} \cdot \frac{d^3}{D^2} \quad (5)$$

where D and H , respectively, represent the splat diameter and splat thickness; Re , the Reynolds number of the impinging particle and d its diameter. In the following calculations, the thickness of the splat was assumed to be equal to 1/12 of the diameter of the impinging particle, as suggested in the literature [3,7].

By rearranging Eq. (5), the diameters of impinging particles having led to the formation of splats were defined as:

$$d = \sqrt{\frac{1}{8}} \cdot D \quad (6)$$

4.6. Probabilistic model

The cumulative distribution of probability of splat equivalent diameters, $G'(x')$, can be correlated with the

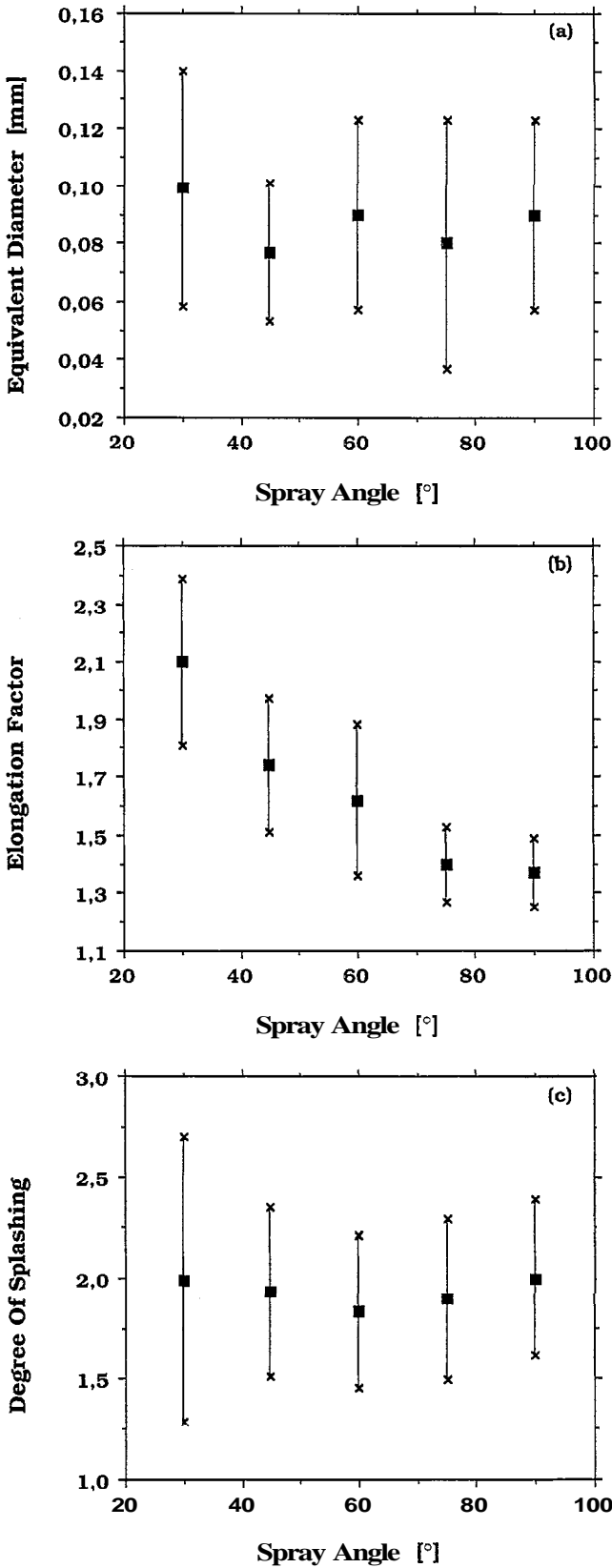


Fig. 7. Flattened particle characteristics, arithmetic average and standard deviation (represented by error bar). (a) Equivalent diameter; (b) elongation factor; (c) degree of splashing.

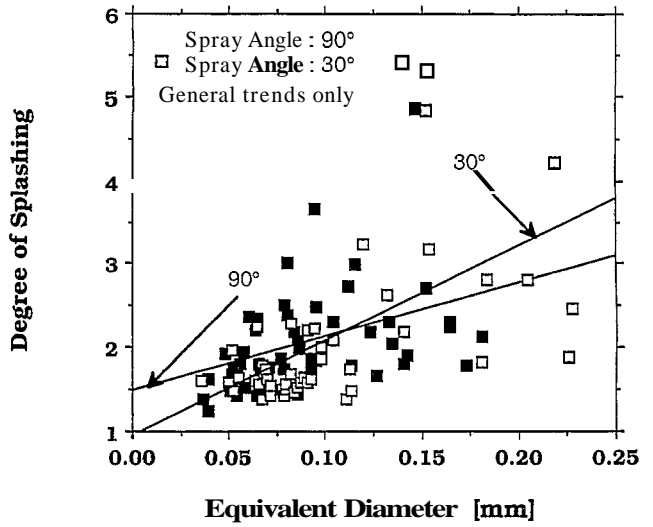


Fig. 8. Evolution of the degree of splashing of splats as a function of their equivalent diameter for 90 and 30° spray angles.

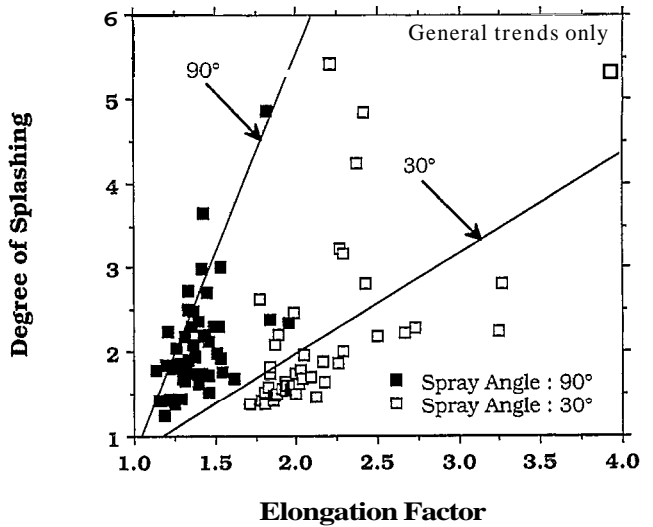


Fig. 9. Evolution of the degree of splashing of splats as a function of the elongation factor for 90 and 30° spray angles.

Table 4

Weibull analysis of equivalent diameter (E.D.), elongation factor (E.F.) and degree of splashing (D.S.) data

Test	E.D.		E.F.		D.S.	
	<i>m</i>	<i>x</i> ₀	<i>m</i>	<i>x</i> ₀	<i>m</i>	<i>x</i> ₀
90°	3.1	0.100	12.4	1.43	5.8	2.16
75°	2.1	0.090	11.4	1.46	5.2	2.06
60°	3.1	0.100	6.9	1.73	5.3	1.99
45°	3.5	0.083	8.3	1.84	5.1	2.10
30°	2.8	0.111	7.8	2.21	3.3	2.24

cumulative distribution of probability of the powder particle sizes, $G(x)$, through a theoretical transfer function (Fig. 10). The diameter of a powder particle, d ,

Table 5
t-test results of the equivalent diameter (E.D.), elongation factor (E.F.) and degree of splashing (D.S.)

Test	90°	75°	60°	45°	30°
90°			E.D.		E.D.
75°			D.S.	E.D.	D.S.
60°					E.D.
45°					D.S.
30°					

Note. The E.D., E.F. and D.S. acronyms in the table indicate similarities (i.e., t value greater than 0.1) between the two data sets indicated.

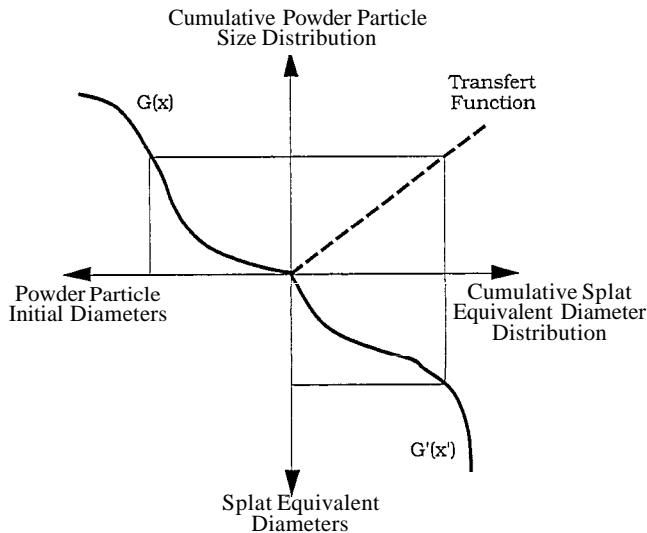


Fig. 10. Basis of the probabilistic model.

which could lead to the formation of an observed splat of equivalent diameter E.D. can be also calculated. As indicated previously, powder particles exhibit near-perfect spherical shapes. The corresponding volume of a particle, V , can therefore be determined. Assuming that the splats present a constant thickness, their thickness can be determined, as well as their degree of flattening.

4.6.1. Results and comparison of methods

Fig. 11 displays the evolution of the extreme calculated values (e.g., smallest and largest diameters) for the different spray angles implementing both approaches (i.e., discrete and probabilistic models). On this graph are also indicated the lower and upper limits of the particle size distribution of the powder; respectively equal to 5 and 88 μm . The two methods induce differences in results. Therefore, the discrete model, based on Madejski's relationship, seems to underestimate the fraction of the particle size distribution which is effectively used to form the splats. This is mainly due to the assumption that the degree of flattening remains constant whatever the initial diameter of the impinging

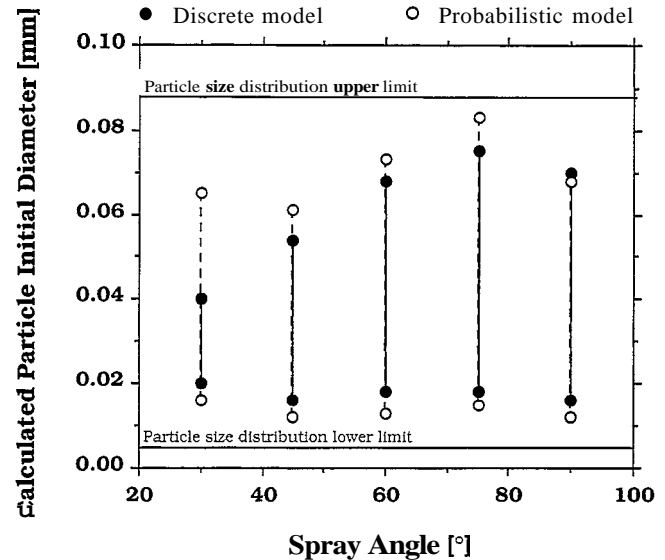


Fig. 11. Variations of the lower and upper limits of the calculated diameters of the powder particles leading to the formation of the splats, for the different spray angles.

particle (ratio taken equal to 1/12 in this specific case). However, the same tendencies are noticed with both models.

To a first approximation, a selected fraction of the particle size distribution is used to form the splats, and this fraction is a function of the spray angle. The fraction of small particles (approximately lower than 15 μm initial diameter) that do not adhere to the substrate is independent of the spray angle. One could therefore assume that these small particles are completely vaporized in the plasma plume (or do not enter the plasma flame) during their flight. On the other hand, the diameter of the largest and unused particles is significantly influenced by the spray angle. To a first approximation, this value remains constant when the angle changes from 90 to 60° and then decreases when the angle decreases to 30°.

Two assumptions may be postulated concerning the behavior of these large particles. On the one hand, they may be partially or even totally unmolten on impact against the substrate and hence rebound at the surface of the substrate. The lower the impact angle, the easier for this phenomenon to occur due to a decrease of the available energy for the particle deformation. On the other hand, the normal velocity of the largest particles can be lower than a minimal velocity (i.e., minimal kinetic energy) necessary to induce the spreading. This will be especially critical when the angle is relatively low (Fig. 12). Thus, at low spray angles, the deposit is built from a more narrow-sized particle size distribution, as shown in Fig. 13; i.e., the deposition efficiency decreases, as experimentally shown in previous papers [8,9].

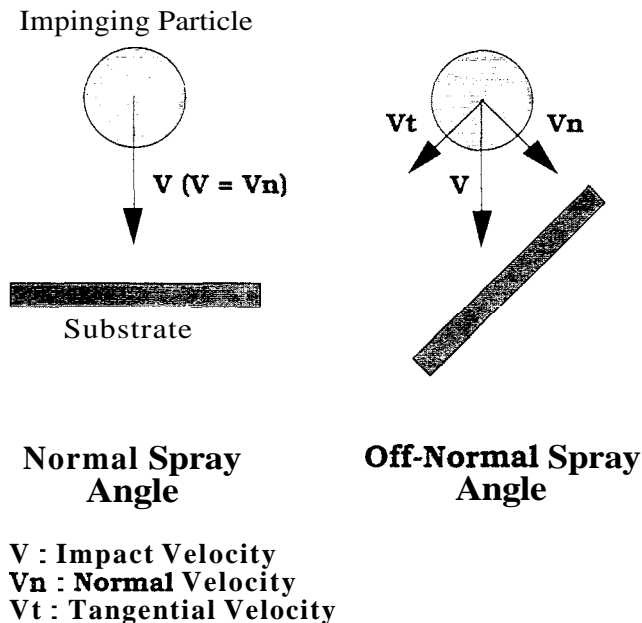


Fig. 12. Schematic illustration of the normal and off-normal angle impact of a molten droplet on a flat substrate.

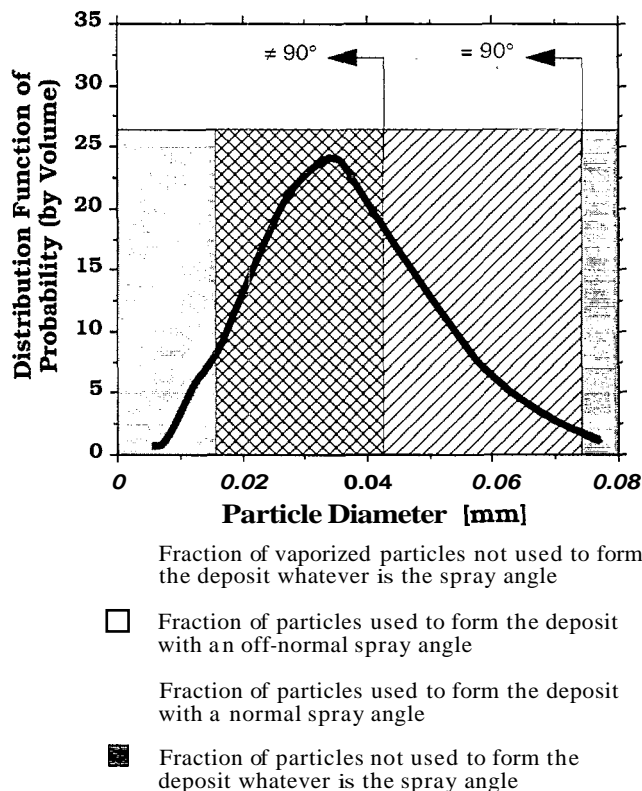


Fig. 13. Particle size distribution of particle leading to the formation of a thermally sprayed deposit for a normal and an off-normal spray angle.

5. Conclusion

Using image analysis, geometric characteristics of individual Astroloy flattened particles deposited onto smooth copper substrates were characterized.

It was shown that the spray angle induces a distortion in the particle morphology, which was characterized by an elongation factor increasing with a decrease of the spray angle. Meanwhile, the degree of flattening, as determined by the equivalent diameter of the splats, is not significantly affected. The splashing phenomenon, characterized through the degree of splashing, becomes more accentuated when the diameter of the impinging particle increases, and secondly when the spray angle decreases.

The diameters of impinging particles leading to the formation of the splats were determined implementing two separate approaches. The first model assumes, for the purpose of the calculations, a constant thickness of the splats equal to 1/12 of the diameter of the impinging particle (i.e., constant degree of flattening). The second model is based on relationships between the particle size distribution and the splat equivalent diameter distribution. The splats result from a selected range of the particle size distribution. The smaller particles seem to be vaporized in the plasma flame during their flight while the largest rebound from the substrate. Thus, the diameter of the largest particles which participate in the formation of the splats decreases when the spray angle decreases. The deposits may be formed at low spray angles from the smaller size fraction of the feedstock and this leads to a reduced deposition efficiency.

NOMENCLATURE

A	area (mm ²)
L	length (mm)
m	Weibull modulus
P	perimeter (mm)
Re	Reynolds number
t	t-test value
x ₀	Weibull characteristic value

Greek letters

μ	arithmetic average (mean value)
σ	standard deviation

Acknowledgement

This study was supported by the French government under grant number MRT 91A0381, by the French companies Turboméca, Société Européenne de

Propulsion and Sochata, and by the NSF Stratman initiative under grant number DDM9215846.

References

- [1] C. Moreau, M. Lamontagne and P. Cielo, in T.F. Bernecki (ed.), *Thermal Spray Research and Applications*, ASM International, Materials Park, OH, USA, 1991, pp. 19–26.
- [2] J.M. Houben, *Relation of the Adhesion of Plasma Sprayed Coatings to the Process Parameters — Size, Velocity and Heat Content of the Spray Particles*, Ph.D. Thesis, Department of Mechanical Engineering, Eindhoven University of Technology, Eindhoven, Holland, December 1988, p. 227.
- [3] S. Fantassi, M. Vardelle, A. Vardelle and P. Fauchais, in C.C. Berndt and T.F. Bernecki (eds.), *Thermal Spray Coatings: Research, Design and Applications*, ASM International, Materials Park, OH, USA, 1993, pp. 81–87.
- [4] C. Moreau, M. Lamontagne and P. Cielo, in T.F. Bernecki (ed.), *Thermal Spray Coatings: Properties, Processes and Applications*, ASM International, Materials Park, OH, USA, 1992, pp. 237–244.
- [5] E. Garrity, D. Wei and D. Apelian, in A.F. Giamei and G.J. Abbaschian (eds.), *Modeling of Casting and Welding Processes IV*, The Minerals, Metals & Materials Society, New York, NY, USA, 1988, pp. 593–602.
- [6] D. Wang, *The Microstructure of Plasma Sprayed Ceramic Coating*, Ph.D. Thesis, Department of Materials Engineering, Monash University, Monash, Australia, March 1991, p. 342.
- [7] H. Liu, E.J. Lavernia and R.H. Rangel, *J. Thermal Spray Technol.*, 2(4) (1993) 369–378.
- [8] M.F. Smith, R. Neiser, R.C. Dykhuizen, in S. Sampath and C.C. Berndt (eds.), *Thermal Spray Industrial Applications*, ASM International, Materials Park, OH, USA, 1994, pp. 603–608.
- [9] G. Montavon, S. Sampath, C.C. Berndt, H. Herman and C. Coddet, in S. Sampath and C.C. Berndt (eds.), *Thermal Spray Industrial Applications*, ASM International, Materials Park, OH, USA, 1994, pp. 469–475.
- [10] G. Montavon, S. Sampath, C.C. Berndt, H. Herman and C. Coddet, *J. Thermal Spray Technol.*, in press.
- [11] X. Chen and E. Pfender, *Plasma Chem. Plasma Process.*, 3(3) (1983) 351–356.
- [12] X. Chen and E. Pfender, *Plasma Chem. Plasma Process.*, 3(2) (1983) 97–114.
- [13] P. Fauchais, A. Vardelle, M. Vardelle, J.F. Coudert and J. Lesinski, *Thin Solid Films*, 121 (1984) 303–316.
- [14] A. Vardelle, (in French) *Etude Numérique des Transferts de Chaleur, de Quantité de Mouvement et de Masse entre un Plasma d'Arc à la Pression Atmosphérique et des Particules Solides*, (Numerical Study of the Heat, Momentum and Mass Transfers between an Atmospheric Plasma and Solid Particles), Ph.D. Thesis, Université de Limoges, Limoges, France, 1987.
- [15] J.M. Houben, in *Proceedings of the 2nd National Conference of Thermal Spray*, Long Beach, CA, USA, 31 October–2 November 1984, ASM International, Materials Park, OH, USA, 1985, pp. 1–12.
- [16] J. Madejski, *Int. J. Heat Mass Transfer*, 19 (1976) 1009–1013.
- [17] G. Trapaga and J. Szekely, *Metallurg. Trans. B*, 22 (1991) 901–914.